Intraplate and interplate earthquakes in Chilean subduction zone: A theoretical and observational comparison

Article *in* Physics of The Earth and Planetary Interiors · June 2009

DOI: 10.1016/j.pepi.2008.03.017

CITATIONS
17

READS
619

4 authors, including:

Felipe Leyton
University of Chile
59 PUBLICATIONS **510** CITATIONS

SEE PROFILE

Javier A. Ruiz
University of Chile
26 PUBLICATIONS **253** CITATIONS

SEE PROFILE

Jaime Campos
University of Chile
101 PUBLICATIONS **2,330** CITATIONS

SEE PROFILE

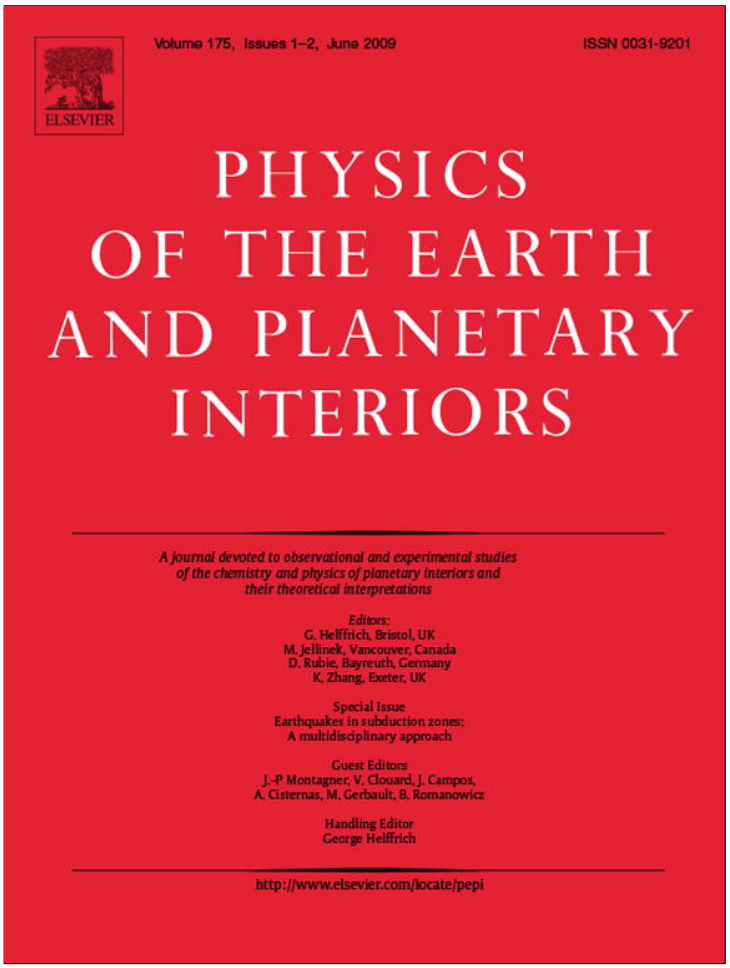

Physics of the Earth and Planetary Interiors 175 (2009) 37–46

Contents lists available at ScienceDirect

Physics of the Earth and Planetary Interiors

journal homepage: www.elsevier.com/locate/pepi

Intraplate and interplate earthquakes in Chilean subduction zone: A theoretical and observational comparison

Felipe Leyton[a,*], Javier Ruiz[b], Jaime Campos[a], Edgar Kausel[a]

[a] Department de Geofísica, Universidad de Chile, Santiago, Chile
[b] Institute du Physic du Globe de Paris, France

ARTICLE INFO

Article history:
Received 3 April 2007
Accepted 3 March 2008

Keywords:
Source parameters
Interplate and intraplate earthquakes
Synthetic waveforms

ABSTRACT

During the last decade, efforts to improve our knowledge of great Chilean earthquakes have shown that not all of the major destructive events have occurred in the contact between the Nazca and south American plates (interplate earthquakes). Waveform analysis of records from the Ms = 8.0, 1950 Antofagasta and the Ms = 7.8, 1939 Chillán earthquakes have shown that these large events are tensional, rupturing along nearly vertical, intermediate depth, fault planes within the subducting slab (intraplate events). Previous studies found that other earthquakes in Chile, like Santiago 1945 (Ms = 7.1), La Ligua 1965 (Ms = 7.1), Tal-tal 1965 (Ms = 6.9), Tocopilla 1970 (Ms = 6.5), and Tarapacá 2005 (Mw = 7.8) were also of tensional type. In the present work, we analyze theoretical and observational evidence comparing interplate and intraplate earthquakes. We found clear differences in the source characteristics between these two kinds of events, with intermediate depth, intraplate earthquakes presenting larger corner frequencies and greater seismic energy release than interplate events (for a given seismic moment). This is also reflected in the higher averaged apparent stress drop for intraplate earthquakes ($\sigma_a \sim 90$ bar) compared to interplate events ($\sigma_a \sim 30$ bar). From theoretical computations, we found that the rupture velocity has a minor effect on the resulting displacements; while directivity and changes in the static stress drop produced notable (and similar) results. We believe that the differences found in the data might be due to changes in the static stress drop, the effect of directivity, or both. Regardless of the cause of the observed differences in the apparent stress drop, these results should be taken into consideration into the assessment of the Seismic Hazard in Chile.

1. Introduction

Chile is located in one of the most active tectonic regions of the world (Scholz, 1990), characterized by the subduction of the Nazca plate under the south American plate at a present rate of 8.0 cm/yr (from NUVEL1 evaluated at 30°S, DeMets et al., 1994) (Fig. 1). The contact between these two plates produces very large earthquakes, with epicenters located along the Chilean coast, depths ranging between 15 and 50 km, known as interplate, thrust events. Recently, seismologist have presented evidence for another kind of earthquakes located in the subducting Nazca plate (Campos, 1989; Campos and Kausel, 1990; Beck et al., 1998; Barrientos et al., 1997), with continental epicenters, intermediate depth (greater than 50 km), known as intraplate or inslab events (Fig. 1). Similar classification has also been found in Mexico's subduction zone (Singh et al., 2000; García et al., 2004), and other subduction zones world-wide (for a review, see Astiz et al., 1988).

Intermediate depth, intraplate events are not exceptional in Chile and have shown considerable destructiveness, causing a great amount of damage and life losses (Kausel, 1991). For example, Chillán, 1939 (Ms = 7.8), with an estimated depth of 80 km (Campos and Kausel, 1990; Beck et al., 1998) destroyed 60% of the housing and caused more deaths than the largest earthquake in the instrumental history: Valdivia, 1960 (Mw = 9.5), an interplate, thrust event. Likewise, Santiago, 1945 (Ms = 7.1), with an estimated depth of 70 km (Barrientos et al., 1997), reached intensities MMI close to VII in the most populated city in Chile, Antofagasta, 1950 (Ms = 8.0) with a depth of 90 km and an epicenter in the border between Chile and Bolivia (Kausel and Campos, 1992), La Ligua, 1965 (Ms = 7.5) with a depth of 70 km (Malgrange et al., 1981), reached intensities between MMI VI and IX, leaving great destruction in Illapel, Combarbalá, La Ligua, Valparaíso, and San Felipe. The Punitaqui, 1997 (Mw = 7.1) event with a depth of 58 km (Pardo et al., 2002; Lemoine et al., 2001) left great losses in the epicentral region. Even more, Astroza et al. (2002) have shown strong differences in the destructiveness between intraplate and

* Corresponding author. Present address: Depto. Ciencias Aplicadas, Universidad de Talca, Curicó, Chile.
E-mail address: felipe@dgf.uchile.cl (F. Leyton).

0031-9201/$ – see front matter © 2009 Elsevier B.V. All rights reserved.
doi:10.1016/j.pepi.2008.03.017

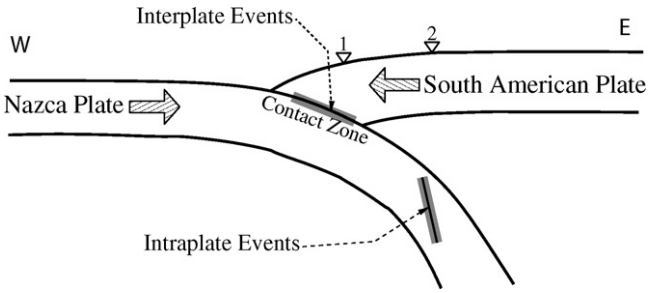

Fig. 1. Schematic cross-section of the subduction in Chile. Large arrows indicate the sense of motions of the plates. Gray areas indicate the location of both kinds of earthquakes studied in this work: interplate and intermediate depth, intraplate. Inverted triangles (1 and 2) indicate the location of stations used in the synthetics seismograms.

intermediate depth, intraplate earthquakes. Indeed, they showed that intraplate earthquakes reach intensities of almost two points in MMI larger than interplate events in the epicentral region, despite the fact that the peak ground accelerations are very similar (Saragoni et al., 2004).

Previous studies (mostly using global, teleseismic data) have shown certain differences between interplate and intraplate earthquakes, specially taking into account the seismic source (Kanamori and Anderson, 1975; Scholz et al., 1986; Kausel and Campos, 1992; García et al., 2004). In the present work, we search for differences between interplate, thrust events and intermediate depth, interplate earthquakes in Chile. We focus on specific source characteristics to make both kinds of events comparable (such as seismic moment, corner frequency, seismic energy, and apparent stress drop) and work with recordings only at regional distances (less than 600 km) to avoid inexactitudes or differences by using regional and teleseismic data (Singh and Ordaz, 1994; Pérez-Campos et al., 2003).

2. Data

We used data from regional recordings of seismic events in central Chile (see Tables 1 and 2, and Fig. 2) that occurred between November, 1999 to January, 2006, magnitudes ranging from 3.5 to 6.5, with a subset of them with known focal mechanisms (from Harvard CMT Project); they were located using the Chilean Seismological Network, shown in white triangles in Fig. 2. We used recording from accelerometers and broadbands with known instrumental response and great dynamic range, enabling the computation of the true ground displacement. We limited the observations to epicentral distances ranging from 50 to 600 km; nevertheless, we also discarded any recording with low signal-to-noise ratio. All traces were sampled at 50 samples per second and, for each one, we removed the instrument response in the frequency domain and filtered with a 2-pole, Butterworth filter between 0.01 and 24 Hz, removing any numerical amplification produced at the lower frequencies due to deconvolution.

Table 1
Location parameters of small, interplate events used in this study.

Code	Date	Latitude	Longitude	Depth (km)
1	11/4/1999	−32.689	−71.715	30.0
2	11/17/1999	−32.707	−71.794	27.1
3	11/17/1999	−32.712	−71.790	25.9
4	11/18/1999	−37.020	−72.650	33.0
5	11/21/1999	−36.490	−72.630	46.0
6	11/28/1999	−32.724	−71.750	27.3
7	12/5/1999	−34.076	−72.349	43.0
8	12/9/1999	−36.323	−72.457	35.4
9	12/9/1999	−36.155	−72.558	33.7
10	12/9/1999	−32.761	−69.185	13.6
11	12/14/1999	−33.264	−68.954	19.1
12	12/20/1999	−36.900	−73.230	33.0
13	12/20/1999	−36.855	−73.463	17.7
14	12/23/1999	−36.970	−73.340	21.4
15	1/27/2000	−33.498	−72.204	40.3
16	2/10/2000	−33.584	−71.967	13.2
17	3/5/2000	−33.107	−71.268	53.8
18	3/26/2000	−32.680	−71.885	13.8
19	3/26/2000	−32.649	−71.875	23.7
20	7/27/2000	−37.240	−73.520	30.0
21	7/27/2000	−37.090	−72.810	33.0
22	8/3/2000	−37.140	−73.880	33.0
23	8/13/2000	−36.340	−72.600	47.0
24	9/3/2000	−35.857	−73.233	35.5

Table 2
Location parameters of small, intermediate depth, intraplate events used in this study.

Code	Date	Latitude	Longitude	Depth (km)
1	11/6/1999	−34.724	−70.957	93.6
2	11/14/1999	−33.175	−70.334	97.8
3	11/20/1999	−37.069	−71.611	134.5
4	12/14/1999	−32.910	−70.048	123.4
5	1/10/2000	−33.197	−70.167	109.1
6	2/2/2000	−34.267	−70.673	101.4
7	2/5/2000	−34.019	−70.978	71.9
8	2/14/2000	−33.081	−70.368	101.2
9	3/5/2000	−33.655	−70.530	102.1
10	3/11/2000	−33.508	−70.872	72.0
11	5/3/2000	−36.330	−72.140	69.0
12	5/5/2000	−36.360	−72.080	69.0
13	5/19/2000	−37.290	−72.420	74.0
14	5/2/2000	−37.680	−71.700	94.0
15	6/20/2000	−39.396	−72.163	88.2
16	8/6/2000	−35.060	−71.170	99.0
17	8/8/2000	−32.740	−70.820	74.0
18	9/9/2000	−36.740	−71.880	92.0
19	8/19/2000	−33.920	−70.260	115.0
20	8/22/2000	−37.064	−72.082	164.4
21	9/5/2000	−33.912	−70.362	121.4
22	9/6/2000	−32.907	−70.371	105.0

The classification criteria into interplate or intermediate depth, intraplate events was defined using the characteristics of the subduction zone in this particular region (Tichelaar and Ruff, 1993; Belmonte-Pool, 1997): it extends down to 45–50 km depth and up to 200 km from the trench (∼100 km from the coast). This broad classification could lead to errors by including events from the accretionary prism in the interplate group. We also analyzed seismicity profiles perpendicular to the trench, as shown in Fig. 3. This figure presents two profiles at (a) 33.5°S and (b) 36.5°S perpendicular to the trench, including all earthquakes within 0.5° North and South; in red are shown the interplate events while in blue are the intermediate depth, intraplate ones. Those with known focal mechanism are plotted with beach balls in cross-section. Note that intraplate events lie right below Santiago (Fig. 3(a)) and Chillán (Fig. 3(b)), 2 very large cities in Chile. Even more, intermediate depth, intraplate events have epicenters that usually lie in highly populated regions: Chilean Central Valley. This feature enhances the importance of our results in the Seismic Hazard assessment in Chile.

3. Methodology

3.1. Source parameters

To compare both kinds of events, we compute source parameters following the work of several authors; here, we do not present the entire derivation, but rather show the most important relations (for more details, see Leyton, 2001). These techniques are based on the

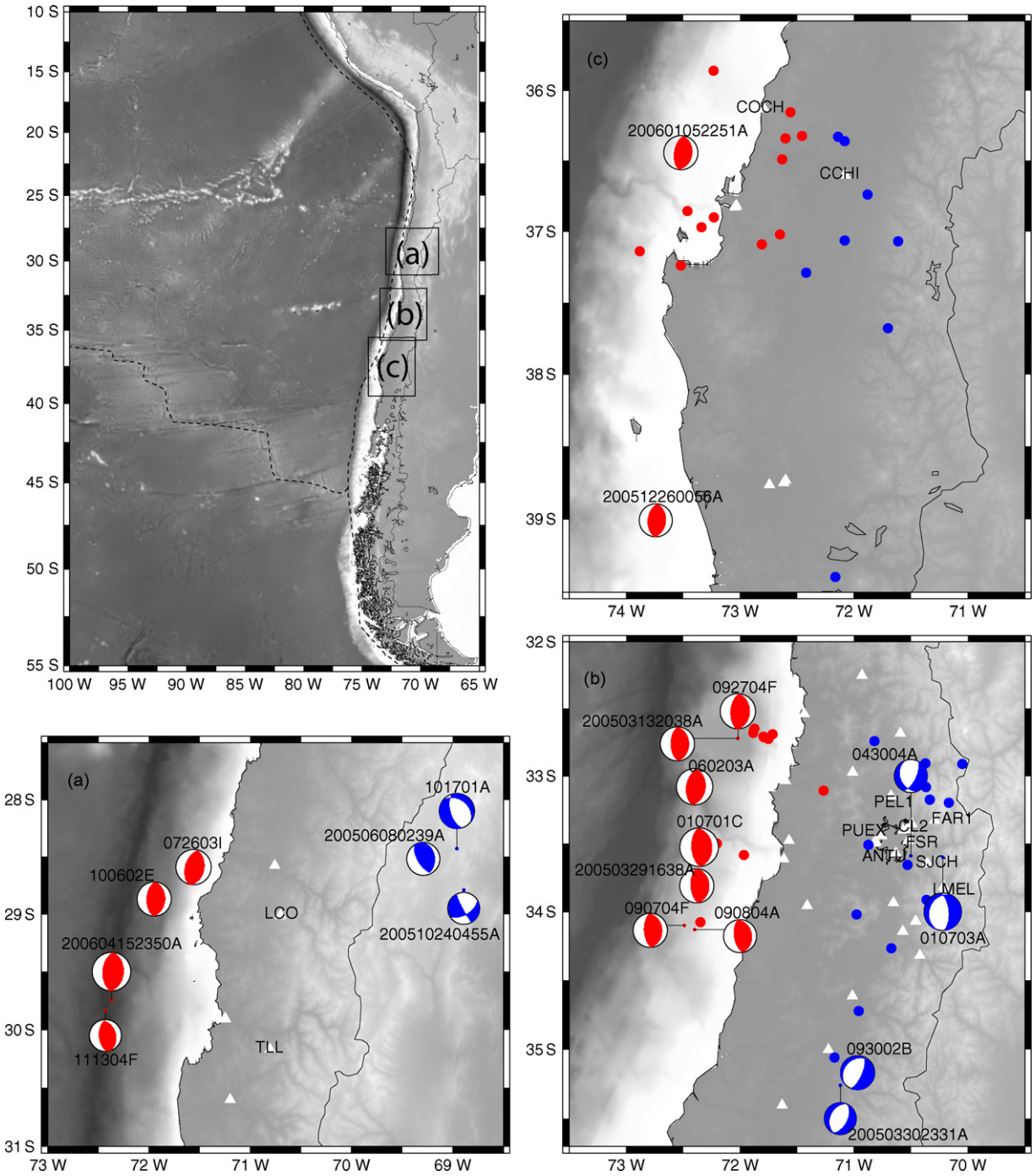

Fig. 2. Maps showing the location of the study and the events used ((a)–(c)). In red we present interplate earthquakes, while in blue, the intermediate depth, intraplate ones. We used beach balls to plot those events with known focal and circles for those without. White triangles mark the position of the Chilean Seismological Network used to locate the events; those with names represent stations used in the waveform analysis (either accelerometers or broadbands with known instrumental response). Labels over beach balls correspond to CMT codes (For interpretation of the references to colour in this figure legend, the reader is referred to the web version of the article.).

analysis of body waves (either compressional P waves or shear S waves), done mostly in the frequency domain; therefore, a crucial point is the isolation of the arrival of a single body wave from the rest of the seismogram.

Firstly, we follow Brune's (1970) work of a simple model for circular seismic source (based on the omega square model of Aki, 1967), commonly used in this kind of studies (Abercrombie, 1995; Ordaz and Singh, 1992; Singh et al., 1999, 2000; Ide and Beroza, 2001; Ide et al., 2003; Kilb et al., 2003; García et al., 2004). Basically, Brune (1970) describes the spectrum of the displacement produced by a seismic source, in the far field ($U(f)$), as:

$$\|U(f)\| = \frac{F^c \mu}{4\pi\rho c^3 G(r)} \cdot \frac{M_0}{1 + (f/f_0)^2}, \quad (1)$$

where F^c represents the radiation pattern, μ is the friction coefficient, ρ and c are the density and wave velocity at the source, respectively, $G(r)$ is the geometrical spreading, with r the hypocentral distance, M_0 is the seismic moment, and f_0 the corner frequency. We include a correction for attenuation and scattering multiplying

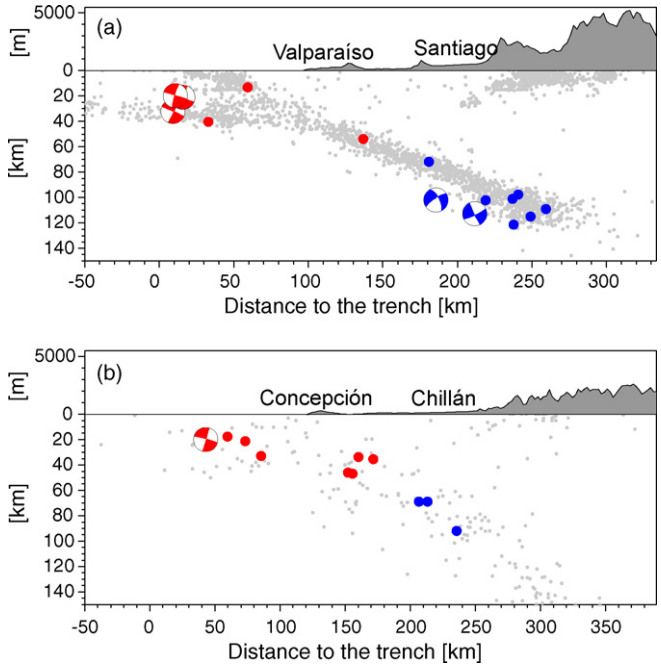

Fig. 3. Cross-section at (a) 33.5°S and (b) 36.5°S showing the events used in this study. In red we present interplate earthquakes, while in blue, the intermediate depth, intraplate ones. We used beach balls (vertical projection) to plot those events with known focal and circles for those without. In light gray is shown the background seismicity recorded from 2000 to 2006 by the Chilean Seismological Service (For interpretation of the references to colour in this figure legend, the reader is referred to the web version of the article.).

the amplitudes by the factor

$$\exp\left(\frac{f\pi r}{Qc}\right), \tag{2}$$

where Q is the attenuation coefficient (Singh et al., 2000).

For the computation of the seismic moment (M_0), we take the limit of the displacement at 0 frequency (Ω)

$$\lim_{f\to 0}\|U(f)\| \equiv \Omega = \frac{F^c\mu}{4\pi\rho c^3 G(r)}M_0. \tag{3}$$

Therefore, to compute the seismic moment (M_0), the corner frequency (f_0), and the attenuation factor (Q) we manually fit Brune's model to the displacement spectrum of a particular body wave. Note that the estimation of corner frequency (f_0) and attenuation factor (Q) is specific for each body wave (either P or S); while the final seismic moment is taken as the average between the estimations made for P and S. An example is shown in Fig. 4, where we present the fit for an event in the frequency domain (bottom); the resulting parameters are shown in the lower right (see figure caption for details). Note how the Brune model is adjusted in the frequency band where the data is above the noise level (between 0.6 and 20 Hz). This process is repeated for each event, independently from its classification (interplate or intraplate), leading to estimations of M_0, f_0, and Q for each one.

Secondly, we evaluate the seismic energy (E_S) released by an earthquake following the methodology described by Boatwright (1980) and Boatwright and Fletcher (1984) based on the computation of the energy flux of a plane wave. Neglecting the effect of directivity, they obtained that

$$E_S = 4\pi C_f^2 r^2 \left(\frac{\langle F^c\rangle}{F^c(\theta,\phi)}\right)^2 \varepsilon_c(x) \tag{4}$$

where C_f represents the free surface coefficient, $\langle F^c\rangle$ is the average of the radiation pattern over the focal sphere (0.52 for I waves and

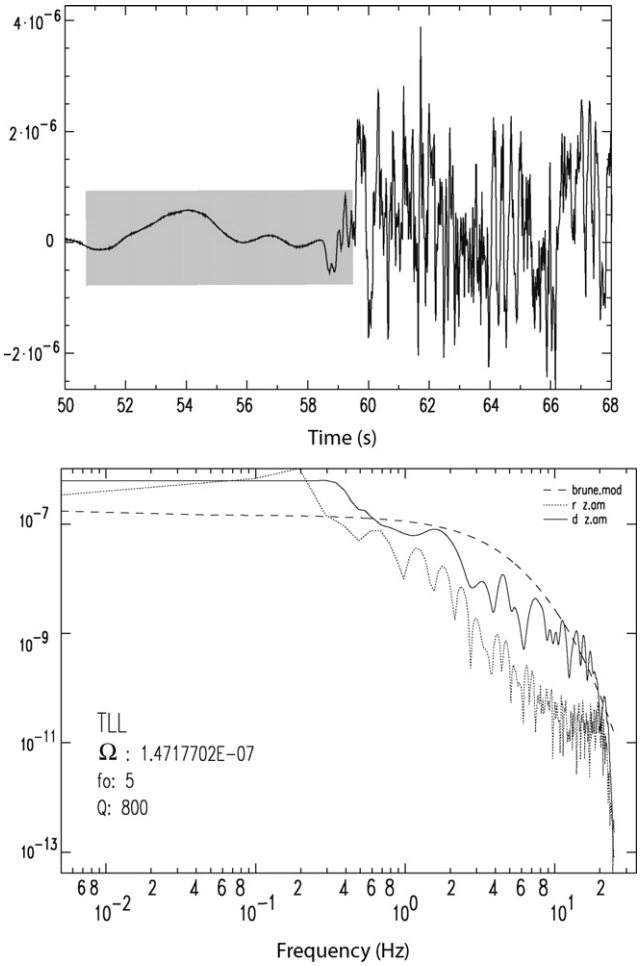

Fig. 4. *Top*: Seismogram of the vertical component recorded in Tololo (TLL), in (m/s); the gray box marks the time window used in the analysis. *Bottom*: Displacement spectrum, in (ms), of the data (solid line), noise (dotted line), and the resulting Brune model (dashed line). The corresponding parameters are shown in the lower right.

0.63 for S waves, from Aki and Richards, 2002), and $\varepsilon_c(x) = \rho c J_c(x)$ is the flux of energy radiated by the seismic wave of velocity c (with the other variables already defined). The most important parameter involved in these computations is J_c (Singh and Ordaz, 1994; Pérez-Campos et al., 2003) defined by Boatwright (1980) as

$$J_c(x) = \int_0^\infty \dot{u}^2(x,t)dt. \tag{5}$$

Snoke (1987) showed a stable way of evaluating $J_c(x)$ by correcting the velocity spectrum known in a limited frequency band, considering Brune's model (Eq. (1)):

$$J_c(x) = 2\int_0^\infty \|V(f)\|^2 df = \frac{2}{3}\|V(f_1)\|^2\cdot f_1 + 2\int_{f_1}^{f_2}\|V(f)\|^2 df + 2\|V(f_2)\|^2\cdot f_2 \tag{6}$$

where $V(f)$ stands for the velocity spectrum and we used Parseval's Theorem. In order to correct for attenuation and scattering, we multiply by the factor described above (Eq. (2)) with its corresponding attenuation coefficient (Q). The process is repeated for both P and S waves, and, finally, the total energy is computed by adding both contributions (Boatwright and Fletcher, 1984; Ide et al., 2003).

An example of these computations is presented in Fig. 5; note the selection of the frequency band where the data is above the noise level, here ranging from $f_1 = 0.2$ Hz and $f_2 = 20$ Hz (Fig. 5(b)),

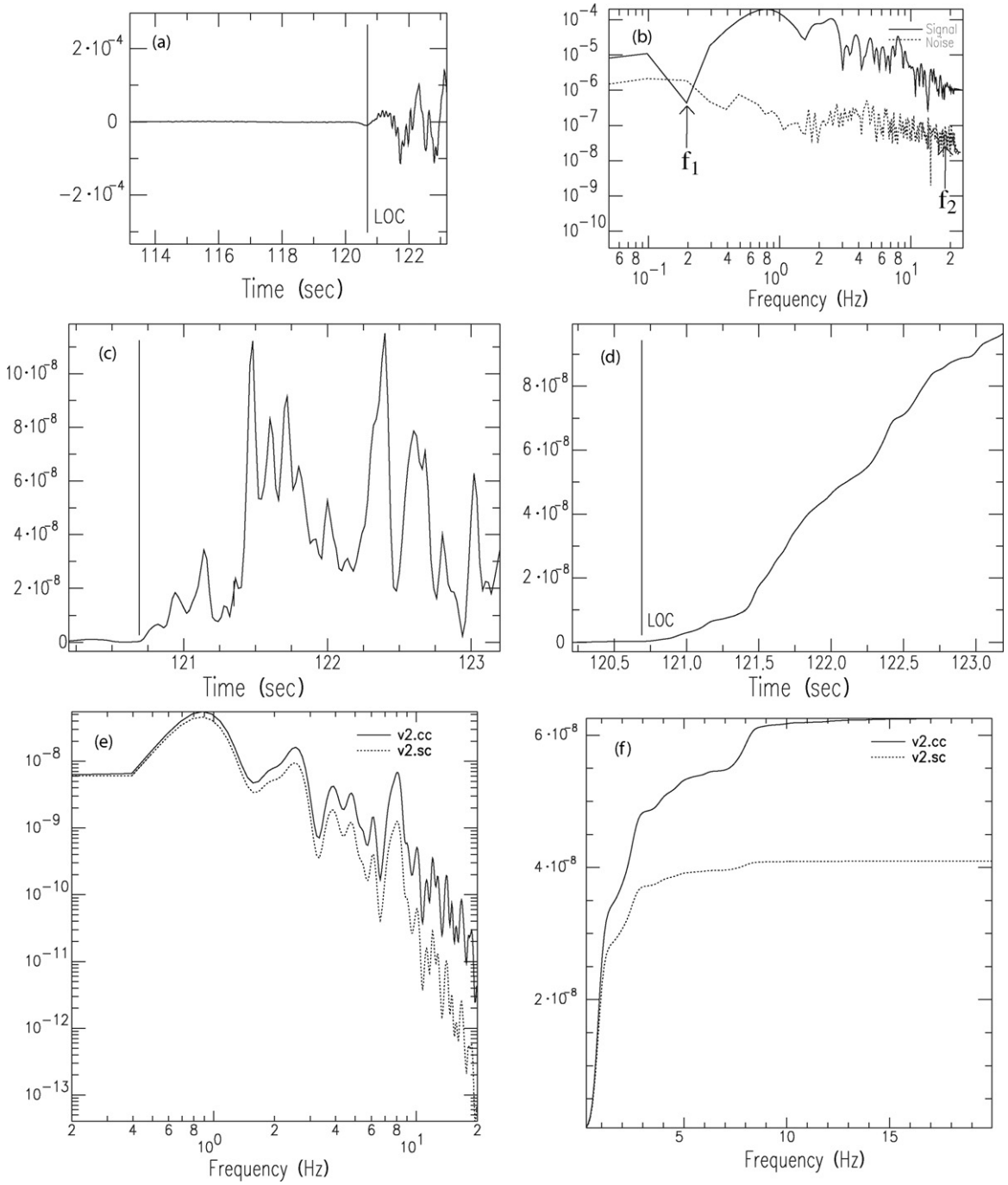

Fig. 5. (a) Vertical component of a seismogram recorded in Calán (CL2), in (m/s). (b) Velocity spectrum of noise (dashed) and data (solid) of the vertical component. (c) Sum of the square of the 3 components, in time. (d) Integral of the sum of the 3 components, in time. (e) Velocity spectrum of the sum of the square of the 3 components, with (solid) and without (dashed) attenuation correction. (f) Integral of the sum of the square of the 3 components, in frequency, with (solid) and without (dashed) attenuation correction.

limits where we do the computations in the frequency domain. We performed the calculations in the time domain (Fig. 5(d)) and frequency domain (Fig. 5(f)) to control the effect of the correction due to attenuation.

Finally, we compute the apparent stress drop (σ_a) following Wyss and Brune (1968):

$$\sigma_a = \mu \frac{E_S}{M_0} \tag{7}$$

in terms of parameters already defined. The apparent stress drop does not have a clear interpretation in terms of physical properties; however, it can be regarded as the energy released per static size of the earthquake (Kanamori and Heaton, 2000). Moreover, considering that $M_0 \sim \langle u \rangle A$ (with $\langle u \rangle$ being the average displacement over the fault and A the total fault area), then

$$\sigma_a \sim E_S/A/\langle u \rangle; \tag{8}$$

hence, σ_a gives an account of the amount of energy released per unit fault area, per unit fault split (Aki, 1966; Wyss and Brune, 1968; Mori et al., 2003; Kanamori and Rivera, 2004).

Table 3
Model parameters used in the computations of synthetics accelerograms.

	Thickness (km)	P wave velocity (km s^{-1})	S wave velocity (km s^{-1})	Density (kg m^{-3})
Layer	50	6.50	3.75	2975
Half space	–	8.16	4.71	3370

Table 4
Source parameters for interplate earthquakes studied here; f_0 is the corner frequency, M_0 the seismic moment, and E_S the seismic energy.

Code	f_0 (Hz)	M_0 (dyne cm)	E_S (erg)	Code	f_0 (Hz)	M_0 (dyne cm)	E_S (erg)
1	1.2	2.082e+23	5.073e+18	20	0.7	2.659e+23	7.278e+18
2	0.7	8.865e+22	4.104e+16	21	0.8	6.474e+22	2.197e+17
3	1.8	4.927e+22	1.451e+18	22	1.0	3.857e+22	1.920e+16
4	1.6	1.174e+23	1.900e+18	23	2.2	1.052e+22	6.088e+17
5	2.7	2.466e+21	9.466e+16	24	1.3	3.562e+22	4.897e+17
6	3.0	6.028e+21	1.148e+17	100602E	0.4	1.150e+24	7.300e+19
7	1.6	9.434e+22	2.816e+18	072603I	0.8	1.600e+23	1.560e+19
8	2.7	1.652e+21	2.220e+16	111304F	1.1	4.160e+22	3.020e+18
9	3.9	8.133e+20	7.192e+16	200604152350A	0.5	1.850e+24	6.980e+19
10	2.6	3.296e+21	3.261e+15	060203A	0.5	1.100e+25	8.690e+20
11	2.8	2.264e+21	4.087e+15	092704F	0.6	3.230e+24	1.940e+20
12	0.5	6.718e+23	6.493e+18	200503132038A	0.5	1.060e+25	3.650e+20
13	1.3	3.812e+22	1.015e+16	090704F	0.4	2.730e+25	8.830e+20
14	0.7	5.065e+23	4.301e+18	090804A	0.6	1.100e+25	1.330e+21
15	1.6	1.593e+23	2.064e+18	010701C	0.2	4.340e+23	3.450e+19
16	2.5	5.592e+21	1.634e+17	200503291638A	0.4	9.210e+24	1.100e+21
17	3.5	6.349e+21	3.650e+16	200601052251A	0.5	1.340e+24	1.260e+20
18	0.5	1.674e+24	3.584e+18	200512260056A	0.8	6.880e+23	6.680e+19
19	3.3	5.125e+21	2.783e+16				

3.2. Theoretical computations

Using an exact discretization in the frequency-wavenumber domain (Bouchon and Aki, 1977; Bouchon, 1979, 1980, 1981), we generated synthetic seismograms considering only intermediate depth, intraplate earthquakes (Fig. 1); we focus our attention on the effect of the rupture velocity, directivity, and stress drop. The source was located at 200 km from the trench (contact between Nazca and south American plates) and at a depth of 65 km; the stations were placed at the surface, 140 and 190 km from the trench, for

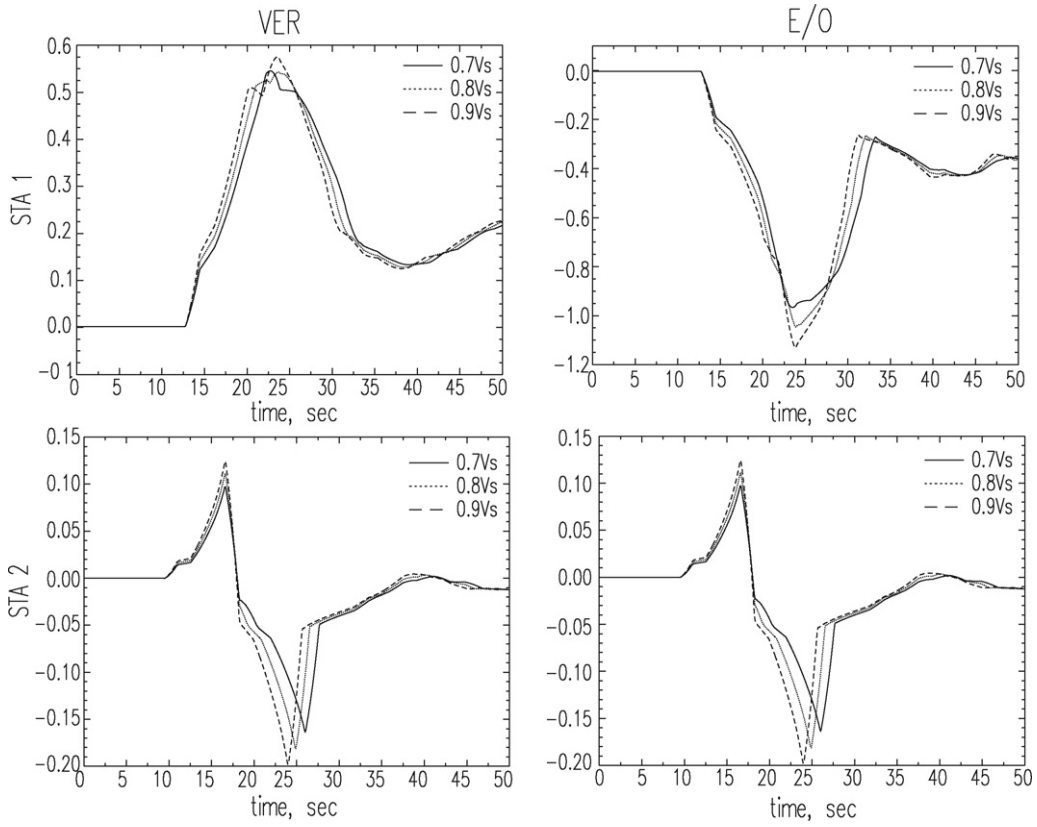

Fig. 6. Synthetics seismograms for an intraplate earthquake (see Fig. 1 and caption for details) with different rupture velocities. On top we present the synthetics at station 1 and on bottom for station 2; while on the left is shown the vertical component and on right the radial. For all of them, kind of line represents a different rupture velocity: in solid is 70%, in dotted is 80%, and in dashed is 90% of the S wave velocity. Amplitudes are normalized to the maximum

Table 5
Source parameters for intermediate depth, intraplate earthquakes studied here; f_0 is the corner frequency, M_0 the seismic moment, and E_S the seismic energy.

Code	f_0 (Hz)	M_0 (dyne cm)	E_S (erg)	Code	f_0 (Hz)	M_0 (dyne cm)	E_S (erg)
1	2.9	3.019e+21	9.687e+16	16	4.5	2.473e+22	3.161e+17
2	3.2	6.754e+21	3.542e+17	17	3.5	1.744e+21	3.229e+16
3	3.5	1.178e+22	1.869e+17	18	5.8	1.290e+21	6.833e+17
4	3.4	1.030e+22	4.141e+17	19	2.5	7.933e+22	5.050e+17
5	3.7	3.104e+22	3.052e+17	20	3.1	1.562e+22	1.188e+18
6	7.2	3.798e+21	5.166e+18	21	4.8	5.159e+21	4.295e+16
7	3.4	4.149e+21	9.776e+16	22	5.1	3.086e+21	9.320e+16
8	3.6	1.219e+22	3.042e+18	101701A	1.4	1.620e+24	2.370e+20
9	4.0	4.618e+22	2.861e+18	200506080239A	1.3	8.120e+23	1.480e+20
10	5.4	5.217e+21	1.230e+18	200510240455A	1.5	2.950e+25	4.680e+21
11	2.9	5.638e+21	9.149e+17	010703A	0.4	2.470e+25	5.490e+21
12	3.7	6.107e+21	7.025e+17	043004A	0.6	1.670e+25	3.380e+21
13	5.1	1.009e+22	6.659e+17	093002B	0.2	8.950e+23	1.240e+20
14	3.5	4.504e+21	6.617e+17	200503302331A	0.9	4.960e+24	1.390e+21
15	5.3	1.421e+22	2.960e+18				

stations 1 and 2, respectively. Note that the stations 1 and 2 (shown in Fig. 1 as inverted triangles) represent the location of main cities in Chile: 1 marks the location of large cities at the coast (such as Valparaíso and Concepción), while 2 marks the locations of cities in the Central Valley (such as Santiago and Chillán), as can be seen from the profiles in Fig. 3. We used a simple model to explore only the effects of the variables mentioned before, presented in Table 3, and the following focal mechanism:

$$\text{strike} = 0^\circ$$
$$\text{dip} = 80^\circ$$
$$\text{rake} = \pm 90^\circ,$$

with -90° for down-dip propagating source and $+90^\circ$ for up-dip propagating source.

The effect of directivity was considered by comparing the displacements produced by a single point source with a set of 3 point sources oriented along the fault's dip, with the rupture front propagating up- or down-dip. Changes in the stress drop were considered by reducing the fault area and increasing the total displacement over the fault, in order to keep the seismic moment constant. Variation in the rupture velocity were considered using an internal parameter that relates it with the S wave velocity. More details can be found in Ruiz (2002).

4. Results

We computed the seismic moment (M_0), corner frequency (f_0), and seismic energy (E_S) from the analysis of body waves in the time and frequency domain, repeating the procedure for each

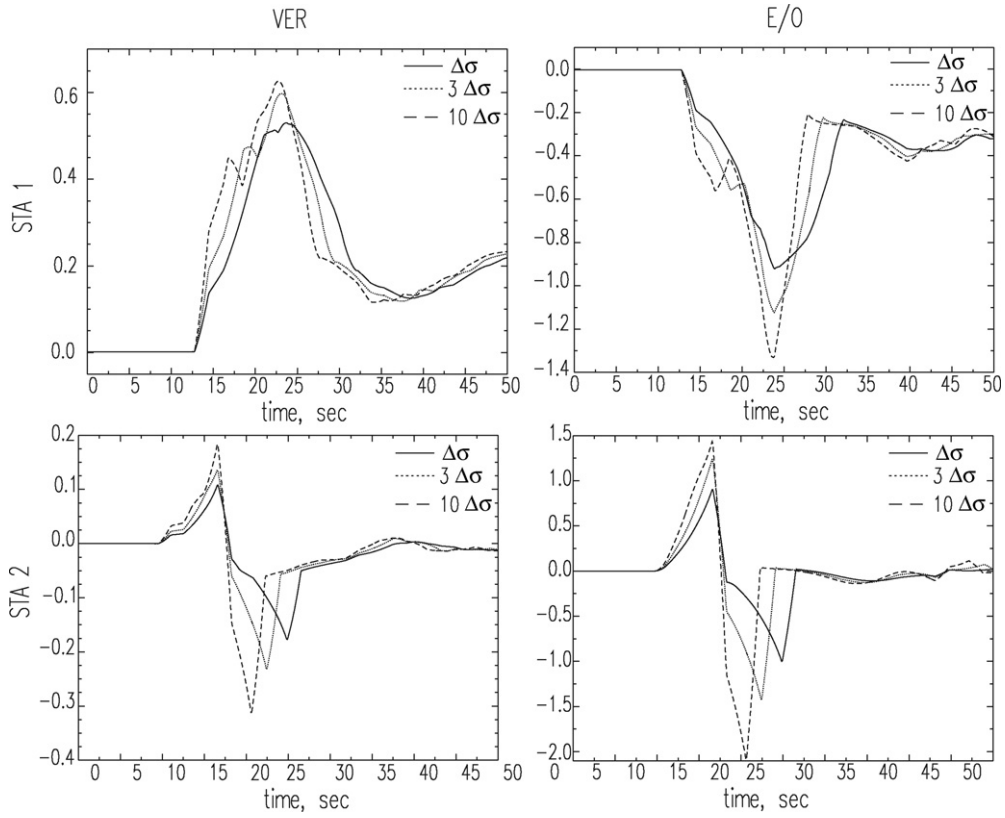

Fig. 7. Synthetics seismograms for an intraplate earthquake (see Fig. 1 and caption for details) with different stress drops. On top we present the synthetics at station 1 and on bottom for station 2; while on the left is shown the vertical component and on right the radial. For all of them, kind of line represents a different stress drop: in solid is $\Delta\sigma$, in dotted is $3\Delta\sigma$, and in dashed is $10\Delta\sigma$. Amplitudes are normalized to the maximum.

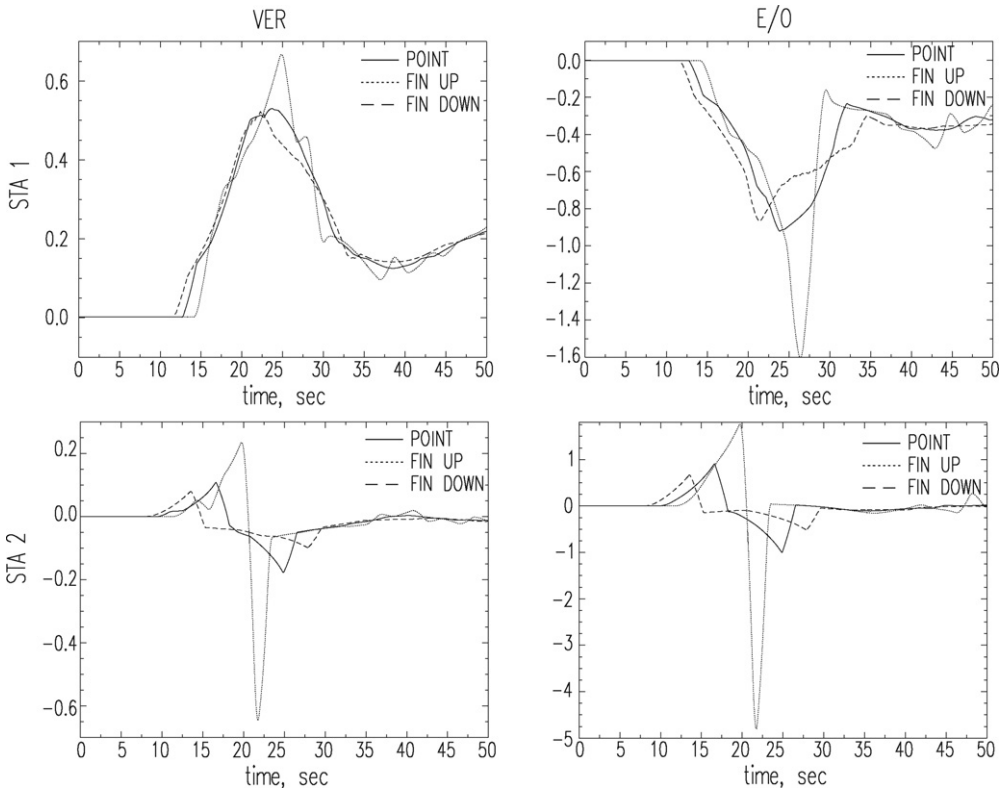

Fig. 8. Synthetics seismograms for an intraplate earthquake (see Fig. 1 and caption for details) with directivity effects. On top we present the synthetics at station 1 and on bottom for station 2; while on the left is shown the vertical component and on right the radial. For all of them, kind of line represents a directivity effect: in solid is the solution for a point source, in dotted is the solution for a finite source rupturing up-dip, and in dashed is the solution for a finite source rupturing down-dip. Amplitudes are normalized to the maximum.

event, regardless of its origin (either interplate or intraplate). The results are presented in Tables 4 and 5 and graphically shown in Figs. 6 and 7, in blue for intraplate events and in red for interplate; note the dispersion of the results, especially for the smaller magnitudes. This might be due to two effects: firstly, errors in the localization of small events causing misclassification of the events into interplate or intraplate (or even the inclusion of earthquakes from the accretionary prism), and secondly, the signal-to-noise ratio and the number of observations is larger for larger events, enabling a better estimation of the source parameters.

Regardless of the scatter in the results, we find a clear differentiation in source parameters between both kinds of

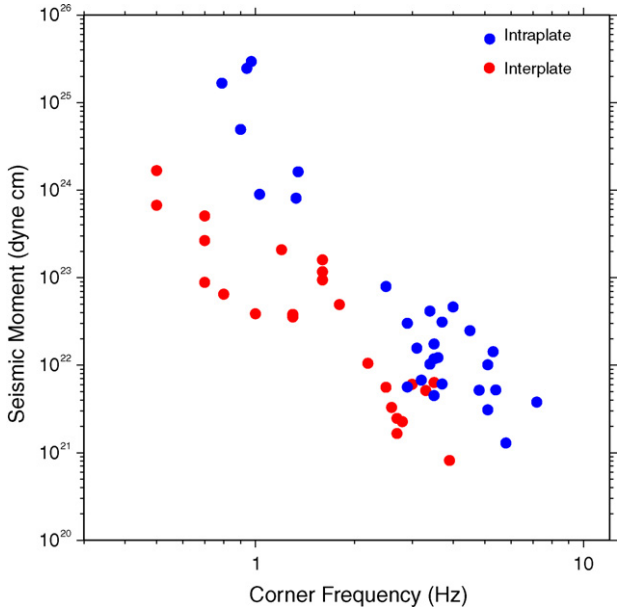

Fig. 9. Relation of seismic moment (M_0) with corner frequency (f_0). In red we present interplate earthquakes, while in blue, the intermediate depth, intraplate ones.

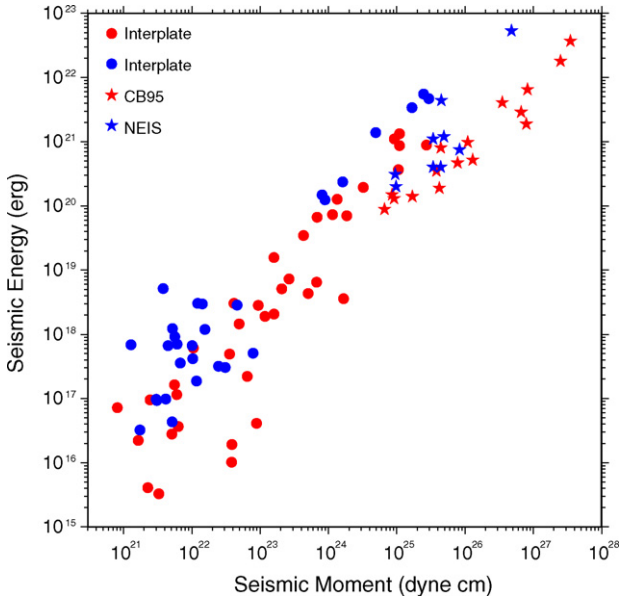

Fig. 10. Seismic energy (E_S) as a function of the seismic moment (M_0). In red we present interplate earthquakes, while in blue, the intermediate depth, intraplate ones. We also show data from Choy and Boatwright (1995) for interplate events and from the USGS (2008) (NEIS) for intermediate depth, intraplate earthquakes in red and blue stars, respectively.

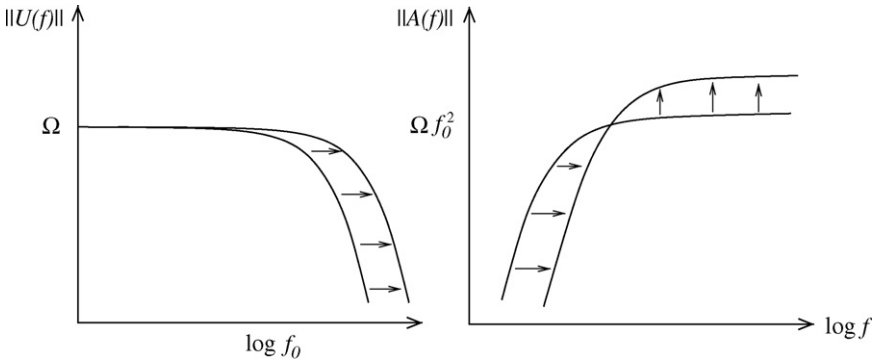

Fig. 11. Brune's Model showing an increase of the corner frequency (f_0), in displacement ($||U(f)||$) and acceleration ($||A(f)||$) spectrums.

events. Indeed, intermediate depth, intraplate events present larger corner frequencies (Fig. 6) and seismic energy (Fig. 7), for a given seismic moment, compared to interplate earthquakes. This is consistent with the idea of differences in the source as suggested by Scholz et al. (1986), where intraplate earthquakes would present a higher frictional strength than interplate earthquakes.

As mentioned earlier, Fig. 6 presents a clear differentiation between both kinds of events: intermediate depth, intraplate earthquakes have larger corner frequencies compared to interplate events. Considering Brune's model, the displacement spectrum for intraplate earthquakes will present more energy in higher frequencies (see Fig. 8) and, in the acceleration spectrum, it will present an increase of the plateau (Ωf_0^2 in Fig. 8). From this result we can conclude that, as an average, the accelerations will be larger for intraplate earthquakes. This effect will produce an increment in the Arias intensity (Arias, 1969) which might explain the large amount of destruction that this kind of events have shown in the past.

Some authors have suggested that the apparent stress drop might increase with magnitude (e.g. Archuleta et al., 1982; Archuleta, 1986; Abercrombie and Leary, 1993; Abercrombie, 1995; Kanamori and Heaton, 2000; Mori et al., 2003); although, recent studies have questioned this result (Ide and Beroza, 2001, 2001; Ide et al., 2003). We tested this hypothesis by comparing our results with those published by Choy and Boatwright (1995) and the USGS (2008) for large earthquakes in the same study region (stars in Fig. 7). We found a great coherency between the behavior of small (Mw ~ 3.0) and large earthquakes (Mw ~ 8.0), especially for interplate events. However, the predicted tendency might be beyond the resolution of the computations presented here (Abercrombie, 1995; Kanamori and Heaton, 2000; Mori et al., 2003). Note that, in the range of seismic moment between 10^{25} and 10^{26} dyne cm, data from Choy and Boatwright (1995) and USGS (2008) lie below ours; we believe that this difference is due to the use of teleseismic versus regional data, as previously reported (Singh and Ordaz, 1994; Pérez-Campos et al., 2003).

We computed synthetics seismograms using an exact discretization in the frequency-wavenumber domain (Bouchon and Aki, 1977; Bouchon, 1979, 1980, 1981) and considered the effect of the rupture velocity, directivity, and stress drop for intermediate depth, intraplate earthquakes (Figs. 9–11). From Fig. 9 we can see that changes in the rupture velocity affect the results only in a minor way; nevertheless, changes in the stress drop and directivity (propagating up-dip) do affect the amplitudes considerably (Figs. 10 and 11). Moreover, their effects are very similar on the synthetics: increase in amplitude and decrease in the duration of the signal, leading to an increase in corner frequency; therefore, the effect of directivity produces an increase in the apparent stress drops, just like a real increase in the static stress drop.

5. Conclusions

We computed some source parameters for a group of events from the Chilean subduction zone, with magnitudes ranging from 3.5 to 6.5, divided into two categories: interplate earthquakes and intermediate depth, intraplate earthquakes. Despite the dispersion in the results, we found a clear difference between both kinds of events. Indeed, intraplate earthquakes show larger corner frequencies and seismic energy release than interplate events, for a given seismic moment (static size).

Comparing our results with those published by Choy and Boatwright (1995) and the USGS (2008), we can conclude that interplate earthquakes (and in a less clear way intraplate events) follow the same behavior in small (Mw ~ 3.5) and large (Mw ~ 8.0) magnitudes, without any apparent tendency to decrease with magnitude, as previously suggested (Abercrombie, 1995; Kanamori and Heaton, 2000; Mori et al., 2003). Therefore, we believe that our results might be extendable to higher magnitudes, even to great earthquakes.

From the synthetics computations, we can conclude that the main effects in the displacements for intermediate depth, intraplate earthquakes come from the directivity effect of an up-dip propagating source and changes in the static stress drop, resulting in an increase in the corner frequency and in the apparent stress drop. Hence, the differences between interplate and intraplate earthquakes observed in this study could be due to directivity, differences in static stress drop, or both. Independently of the cause, intermediate depth, intraplate events present larger release of seismic energy per static size of the event (seismic moment) compared to interplate earthquakes. These results have a great significance for the assessment of the Seismic Hazard in Chile because a different kind of earthquake has to be taken into account, especially for large cities located in the Central Valley.

Acknowledgments

We would like to thank the Chilean Seismological Service and the Harvard CMT Project for making their data available. We also thank R. Madariaga and M. Astroza for encouraging discussions, and B. Romanowicz and G. Beroza for their insightful review and constructive comments that greatly improved this manuscript. We are very grateful to O. Coutant for making his code available to us. This work was funded by the Millennium Nucleus in Seismotectonics and Seismic Hazard, Fondecyt contract 11070030, and supported by Conicyt-ECOS. Most figures were made using GMT (Wessel and Smith, 1991) and some computations used SAC (Goldstein et al., 1995).

References

Abercrombie, R., 1995. Earthquake source scaling relationships from −1 to 5 M_L using seismograms recorded at 2.5 km depth. J. Geophys. Res 100, 24015–24036.

Abercrombie, R., Leary, P., 1993. Source parameters of small earthquakes recorded at 2.5 km depth, Cajon Pass, southern California: implications for earthquake scaling. Geophys. Res. Lett. 20, 1511–1514.

Aki, K., 1966. Generation and propagation of G waves from the Niigata earthquake of June 16, 1964. part 2. estimation of earthquake moment, from G wave spectrum. Bull. Earth Res. Inst. 44, 73–88.

Aki, K., 1967. Scaling law of seismic spectrum. J. Geophys. Res. 72, 1217–1231.

Aki, K., Richards, P.G., 2002. Quantitative Seismology. University Science Books, Sausalito, California.

Archuleta, R.J., 1986. Downhole recordings of seismic radiation. In: Earthquake Source Mechanics. Geophys. Monogr. Ser., vol. 37. AGU, Washington, DC, pp. 311–318.

Archuleta, R.J., Cranswick, C., Mueller, C., Spudich, P., 1982. Source parameters of the 1980 Mammoth Lakes, California, earthquake sequence. J. Geophys. Res. 87, 4595–4607.

Arias, A., 1969. Measure of Earthquake Intensity. Massachusetts Institute of Technology, Cambridge.

Astiz, L., Lay, T., Kanamori, H., 1988. Large intermediate-depth earthquakes and the subduction process. Phys. Earth Planet. Inter. 53, 80–166.

Astroza, M., Sandoval, M., Kausel, E., 2002. Estudio comparative de los efectos de los sismos chilenos de subducción del tipo intraplaca de profundidad intermedia. In: Congreso Chileno de Sismología e Ingeniería Antisísmica.

Barrientos, S., Kausel, E., Campos, J., 1997. Sismicidad de profundidad intermedia y peligro sísmico en Santiago. In: VII Congreso Geológico de Chile, Antofagasta. Soc. Geolog. Chilena, pp. 645–649.

Beck, S., Barrientos, S., Kausel, E., Reyes, M., 1998. Source characteristics of historic earthquakes along the central Chile subduction zone. J. South Am. Earth Sci. 11, 115–129.

Belmonte-Pool, J., 1997. Análisis del contacto sismogénico interplaca a lo largo de chile. Memoria para optar al grado de Magister en Ciencias, mención Geofísica. Universidad de Chile.

Boatwright, J., 1980. A spectral theory for circular seismic sources; simple estimates of source dimension, dynamic stress drop and radiated seismic energy. Bull. Seismol. Soc. Am. 70, 1–27.

Boatwright, J.L., Fletcher, J.B., 1984. The partition of radiated energy between P and S waves. Bull. Seismol. Soc. Am. 74, 361–375.

Bouchon, M., 1979. Discrete wave number representation of elastic wave fields in three-space dimensions. J. Geophys. Res. 84, 3609–3614.

Bouchon, M., 1980. Calculation of complete seismograms for an explosive source in a layered medium. Geophysics 45, 197–203.

Bouchon, M., 1981. A simple method to calculate Green's functions for elastic layered media. Bull. Seismol. Soc. Am. 71, 959–971.

Bouchon, M., Aki, K., 1977. Discrete wave-number representation of seismic source wave fields. Bull. Seismol. Soc. Am. 67, 259–277.

Brune, J.N., 1970. Tectonic stress and spectra of seismic shear waves from earthquakes. J. Geophys. Res. 75, 4997–5009.

Campos, J., 1989. Determinación de parámetros focales por medio de modelamiento de ondas de cuerpo del sismo del 9 de diciembre de 1950. Memoria para optar al grado de Magister en Ciencias, mención Geofísica. Universidad de Chile.

Campos, J., Kausel, E., 1990. The large intraplate earthquake of southern Chile. Seism. Res. Lett. 61, 43.

Choy, G.L., Boatwright, J.L., 1995. Global patterns of radiated seismic energy and apparent stress. J. Geophys. Res. 100, 18205–18228.

DeMets, C., Gordon, R., Argus, D., Stein, S., 1994. Effect of recent revision to the geomagnetic reversal time scale on estimates of current plate motion. Geophys. Res. Lett. 21, 2191–2194.

García, D., Singh, S.K., Herráiz, M., Pacheco, F.J., Ordaz, M., 2004. Inslab earthquakes of central Mexico: *Q*, source spectra, and stress drop. Bull. Seismol. Soc. Am. 94, pp. 789–202.

Goldstein, P., Dodge, D., Firpo, M., 1995. SAC—Seismic Analysis Code. URL http://www.llnl.gov/sac/.

Ide, S., Beroza, G.C., 2001. Does apparent stress vary with earthquake size? Geophys. Res. Lett., 28.

Ide, S., Beroza, G.C., Prejean, S.G., Ellsworth, W.L., 2003. Apparent break in earthquake scaling due to path and site effects on deep borehole recordings. J. Geophys. Res., 108.

Kanamori, H., Anderson, D.L., 1975. Theoretical basis of some empirical relations in seismology. Bull. Seismol. Soc. Am. 65, 1073–1095.

Kanamori, H., Heaton, T.H., 2000. Microscopic and macroscopic physics of earthquakes. In: Rundle, J., Turcotte, D.L., Klein, W. (Eds.), Geocomplexity and the Physiscs of Earthquakes. American Geophysical Union, Washington, DC, pp. 147–163.

Kanamori, H., Rivera, L., 2004. Static and dynamic scaling relations for earthquakes and their implications for rupture speed and stress drop. Bull. Seismol. Soc. Am. 94, 314–319.

Kausel, E., 1991. The influence of large thrust and normal earthquake in the assessments of the seismic hazard. In: Workshop "New Horizons in the Strong Motion: Seismic Studies and Engineering Practice". Santiago, Chile, 4–7 de junio de 1991 (abstract).

Kausel, E., Campos, J., 1992. The M_S = 8 tensional earthquake of 9 December 1950 of northern Chile and its relation to the seismic potencial of the region. Phys. Earth Planet. Inter. 72, 220–235.

Kilb, D., Biasi, G., Brune, J., Anderson, J., Vernon, F.L., 2003. Quantifying properties of seismic spectra: an examination of 100's of spectra from southern California earthquakes recorded by the ANZA seismic network. AGU Fall Meeting Abstracts, C173+.

Lemoine, A., Madariaga, R., Campos, J., 2001. Evidence for earthquake interaction in the Illapel gap of central Chile. Geophys. Res. Lett. 28, 2743–2746.

Leyton, F., 2001. Estudio comparativo de eventos inter e intraplaca desde el punto de vista sismológico en Chile. Memoria para optar al grado de Magister en Ciencias, mención Geofísica. Universidad de Chile.

Malgrange, M., Deschamps, A., Madariaga, R., 1981. Thrust and extensional faulting under the chilean coast: 1965 and 1971 Aconcagua earthquake. Geophys. J. R. Astron. Soc. 66, 313–332.

Mori, J.J., Abercrombie, R.E., Kanamori, H., 2003. Stress drops and radiated energies of the Northridge aftershocks. J. Geophys. Res., 108.

Ordaz, M., Singh, S.K., 1992. Source spectra and spectral attenuation of seismic waves from Mexican earthquakes, and evidence of amplification in the hill zone of Mexico City. Bull. Seismol. Soc. Am. 82, 24–43.

Pardo, M., Comte, D., Monfret, T., Boroschek, R., Astroza, M., 2002. The October 15,1997 Punitaqui earthquake (Mw = 7.1): a destructive event within the Nazca plate in central Chile. Tectonophysics 345, 199–210.

Pérez-Campos, X., Singh, S.K., Beroza, G.C., 2003. Reconciling teleseismic and regional estimates of seismic energy. Bull. Seismol. Soc. Am. 93, 2123–2130.

Ruiz, J., 2002. Efectos sismogénicos en los movimientos fuertes del suelo para sismos chilenos: aspectos teóricos y observaciones. Memoria para optar al grado de Magister en Ciencias, mención Geofísica. Universidad de Chile.

Saragoni, R., Astroza, M., Ruiz, S., 2004. Comparative study of subduction earthquake ground motion of north, central, and south America. In: 13th World Conference on Earthquake Engineering. Vancouver, BC, Canada, August 1–6, 2004.

Scholz, C.H., 1990. The Mechanics of Earthquakes and Faulting. Cambridge University Press.

Scholz, C.H., Aviles, C.A., Wesnousky, S.G., 1986. Scaling differences between large interplate and intraplate earthquakes. Bull. Seismol. Soc. Am. 76, 65–70.

Singh, S.K., Ordaz, M., 1994. Seismic energy release in Mexican subduction zone earthquakes. Bull. Seismol. Soc. Am. 84, 1533–1550.

Singh, S.K., Ordaz, M., Alcántara, L., Shapiro, N., Kostoglodov, V., Pacheco, J.F., Alcocer, S., Guitiérrez, C., Quass, R., Mikumo, T., Ovando, E., 2000. The Oaxaca earthquake of 30 septembre 1999 (Mw = 7.5): a normal-fault event in the subducted Cocos Plate. Seism. Res. Lett. 71, 67–78.

Singh, S.K., Ordaz, M., Pacheco, J.F., Quass, R., Alcántara, L., Alcocer, S., Guitiérrez, C., Meli, R., Ovando, E., 1999. A preliminary report on the Tehuacan, Mexico earthquake of June 15, 1999, (Mw = 7.0). Seism. Res. Lett. 70, 489–504.

Snoke, J.A., 1987. Stable determination of (Brune) stress drops. Bull. Seismol. Soc. Am. 77, 530–538.

Tichelaar, B.W., Ruff, L.J., 1993. Depth of seismic coupling along the subduction zone. J. Geophys. Res. 98, 2017–2037.

USGS, 2008. Source parameter search result. URL http://neic.usgs.gov/neis/sopar/.

Wessel, P., Smith, W.H.F., 1991. Free software helps map and display data. EOS Trans. AGU 72, 441.

Wyss, M., Brune, J.N., 1968. Seismic moment, stress, and source dimensions for earthquakes in the California-Nevada region. J. Geophys. Res. 73, 4681–4694.